Sexual attraction in the silkworm moth: structure of the pheromone-binding-protein–bombykol complex

Benjamin H Sandler[1], Larisa Nikonova[2], Walter S Leal[2] and Jon Clardy[1]

Background: Insects use volatile organic molecules to communicate messages with remarkable sensitivity and specificity. In one of the most studied systems, female silkworm moths (*Bombyx mori*) attract male mates with the pheromone bombykol, a volatile 16-carbon alcohol. In the male moth's antennae, a pheromone-binding protein conveys bombykol to a membrane-bound receptor on a nerve cell. The structure of the pheromone-binding protein, its binding and recognition of bombykol, and its full role in signal transduction are not known.

Results: The three-dimensional structure of the *B. mori* pheromone-binding protein with bound bombykol has been determined by X-ray diffraction at 1.8 Å resolution.

Conclusions: The pheromone binding protein of *B. mori* has six helices, and bombykol binds in a completely enclosed hydrophobic cavity formed by four antiparallel helices. Bombykol is bound in this cavity through numerous hydrophobic interactions, and sequence alignments suggest critical residues for specific pheromone binding.

Addresses: [1]Department of Chemistry and Chemical Biology, Cornell University, Ithaca, NY 14853-1301, USA. [2]Laboratory of Chemical Prospecting, National Institute of Sericultural and Entomological Sciences, 1-2 Ohwashi, Tsukuba Science City 305-8634, Japan.

Correspondence: Jon Clardy
E-mail: jcc12@cornell.edu

Key words: chemical communication, insect pheromone, molecular recognition, odorant-binding protein, X-ray crystallography

Received: **13 December 1999**
Accepted: **21 December 1999**

Published: **19 January 2000**

Chemistry & Biology 2000, **7**:143–151

1074-5521/00/$ – see front matter

Introduction

Insects largely perceive the world through chemistry [1,2]. For many insects, small-molecule signals regulate such fundamental behaviors as eating, mating and egg laying, and they have macromolecular systems of extraordinary specificity and sensitivity to detect these signals [2]. One of the best-studied systems is reproductive signaling in lepidoptera — the moths and butterflies [3,4].

Mature moths exist to reproduce — they typically do not even eat during their short lifetimes — and successful reproduction begins by locating a partner of the opposite sex. Female moths 'call' potential mates by releasing volatile sex pheromones [2–4]. The first sex pheromone to be chemically characterized, (E,Z)-10,12-hexadecadienol or bombykol, was from the silkworm moth (*Bombyx mori*), and Butenandt's classic structure elucidation of bombykol appeared over 40 years ago (Figure 1) [5,6]. Electrophysiological recordings from male *B. mori* antennae indicate single-molecule sensitivity for bombykol — the theoretical detection limit for chemical communication [7]. A male moth's pheromone detection system also requires a fast response time in order to follow a turbulent wind-borne pheromone trail, and experimental values of 0.5 seconds have been reported [8]. The molecular mechanisms underlying this impressive chemical sensor are not known, but growing evidence suggests a highly collaborative effort by various olfactory specific proteins, including pheromone receptors, pheromone-binding proteins and pheromone-degrading enzymes.

A male moth senses chemical signals with his antennae, which are covered with olfactory 'hairs' called sensilla. A male silkworm moth's antennae contain 15,000–20,000 sensilla, half of which are specialized for the detection of bombykol [2]. Sensilla contain extensions from dendritic receptor cells, and receptors in the dendritic membranes transduce the extracellular chemical signal into intracellular second messengers [1]. Bombykol enters sensilla through microscopic openings in the waxy cuticle surrounding them. These microscopic pores are thought to provide physical access for airborne odorants, while minimizing evaporation of the aqueous solution (sensillary lymph) that surrounds the dendritic receptor cells. The hydrophobic pheromone must pass through the

Figure 1

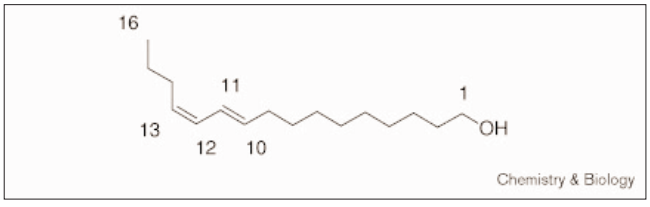

The chemical structure of bombykol.

Figure 2

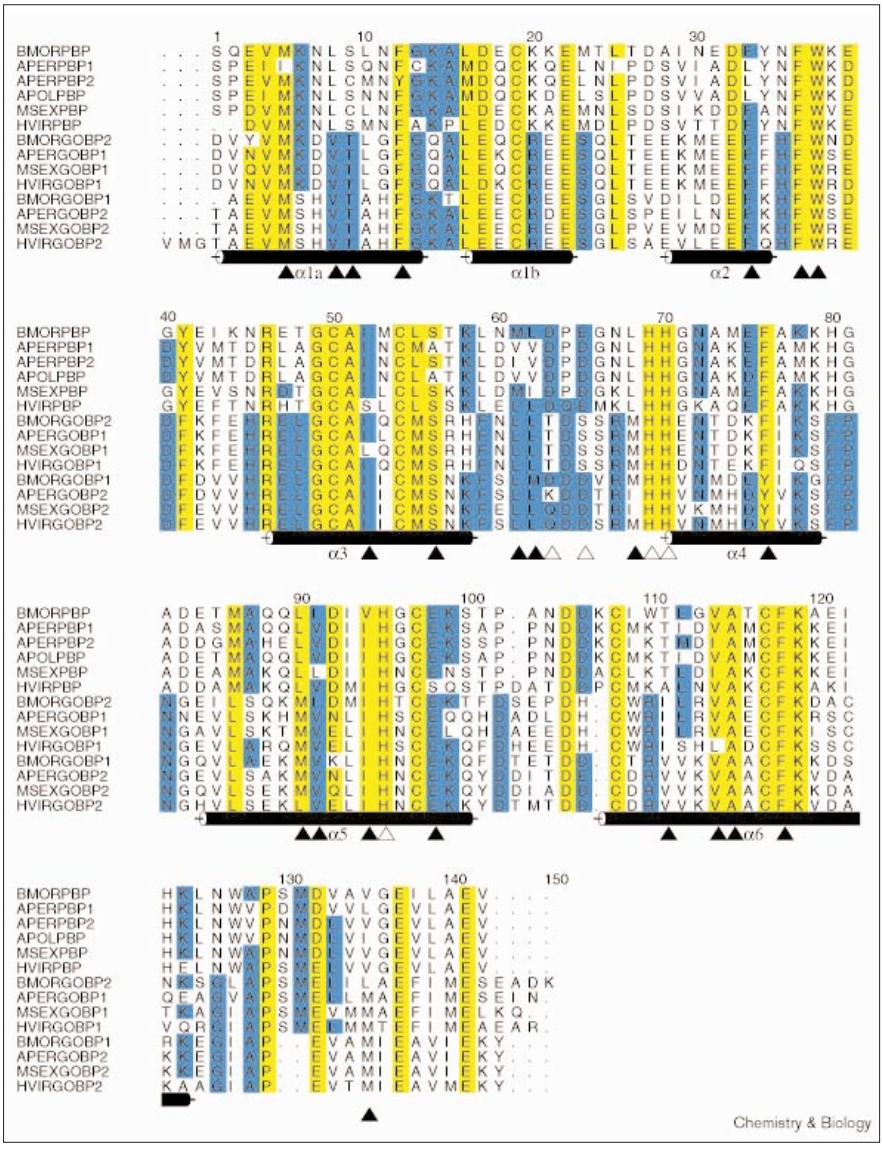

Sequence alignment of the lepidopteran pheromone-binding proteins (PBP) and general odorant binding proteins (GOBP). BMOR, *B. mori*; APER, *Antheraea pernyi*; APOL, *Antheraea polyphemus*; MSEX, *Manduca sexta*; HVIR, *Heliothis virescens*. Black triangles indicate residues involved in the hydrophobic binding pocket and open triangles are involved in a putative pH-sensitive conformational change (see text). Residues in yellow have high (> 90%) consensus value, whereas residues in blue have a lower (> 50%) consensus value. Sequence alignment and homology calculations were performed in MULTALIN [34] using default settings and data from SWISPROT. The figure was prepared with ALSCRIPT [35].

sensillary lymph to interact with the membrane-bound pheromone receptor, and this passage requires the participation of a pheromone-binding protein [9]. Pheromone-binding proteins (PBPs) are small — typically less than 20 kDa — water-soluble proteins that occur in high abundance — typically 10 mM — in the sensillary lymph of male antennae [9].

Molecular cloning has identified PBPs as a subfamily of the odorant-binding protein (OBP) family in several insect species [9]. The PBP family is predominantly expressed in male antennae and localized in pheromone-sensitive sensilla [9,10]. The other two families of general odorant-binding proteins (GOBPs) are found in both male and female antennae and are localized in sensilla that respond to food and host odors [9,10]. *B. mori*, for example, has one PBP and at least two GOBPs, which are included in the multiple alignment diagram of lepidopteran OBPs (Figure 2) [11]. In general the PBPs from different moth species have ~60% sequence identity, whereas the PBP subfamily has a lower degree of sequence identity — typically 30% — with the GOBP subfamily [12]. Binding studies demonstrate that the interactions between pheromones and PBPs are specific and selective [12,13].

In this paper we report the results of a single crystal X-ray diffraction analysis of the PBP of *B. mori* complexed with bombykol that characterizes, for the first time, the three-dimensional structure of a PBP and outlines the molecular determinants of pheromone-binding specificity.

Results and discussion

Overall architecture of *B. mori* PBP

The 15.9 kDa *B. mori* PBP was expressed in *Escherichia coli* and structurally characterized by single crystal X-ray diffraction analysis [12,14]. It has approximate dimensions of $40 \times 35 \times 30$ Å, formed by a roughly conical arrangement of six α helices (Figure 3). Four antiparallel helices (α1, α4, α5 and α6) converge to form the binding pocket. The converging ends of the helices form the narrow end of the pocket, and the pocket's opposite end is capped by another helix, α3 (Figure 3). Disulfide bonds and helix–helix packing enforce the organization of the helices. Two disulfide bonds (Cys19–Cys54 and Cys50–Cys108) fix the relative position of α3 by attaching it to the flanking helices α1 and α6. Another disulfide (Cys97–Cys117) bridges helices α5 and α6, further rigidifying the protein (Figure 3). All six cysteine residues are completely conserved in lepidopteran OBPs (Figure 2). The disulfide structures of recombinant and native PBP have been determined by analytical methods [15].

Helices α4 and α5 pack in a classic knobs-into-holes fashion, although the packing angle, 35°, deviates from the ideal 20°. Residues Ala73, Met74 and Ala77 of α4 and Ala87, Leu90 and Ile91 of α5 pack in this fashion, and all of the alanine residues are conserved in lepidopteran PBPs (Figure 2). Helices α5 and α6 pack in a ridges-into-grooves fashion with a 50° packing angle using residues Ile93, Val94 and Cys97 of α5 and Cys117, Phe118 and Glu121 of α6 to form a hydrophobic assembly in the contact region. The remaining helices pack together irregularly and with small interhelix contacts. Helices α1 and α3 pack at an angle of 65° with a hydrophobic interaction between Met23 (α1), Cys50 and Cys54 (α3), and an electrostatic interaction between Glu22 (α1) and Lys58 (α3). Helices α2 and α3 pack at an angle of 65°, with a tiny hydrophobic core of Leu16 and Phe33 (α2) and Thr48, Ile52 and Leu55. Helices α3 and α6 cross at 85° with Gly49, Ile52 and Met53 (α3) interacting with Cys108 and Thr111 (α6). The fold of *B. mori* PBP is completely different from the β-barrel fold observed in vertebrate OBPs [16].

The surface of *B. mori* PBP is, not surprisingly for such a soluble protein, covered with charged residues — 21 glutamate or aspartate residues and 14 lysine or arginine residues. The crystallographic asymmetric unit of PBP contains two monomers, and as Campanacci *et al.* [17] have reported that the *Mamestra brassicae* PBP is dimeric at physiological concentrations, the solid-state structure of *B. mori* PBP was analyzed for possible insights into

Figure 3

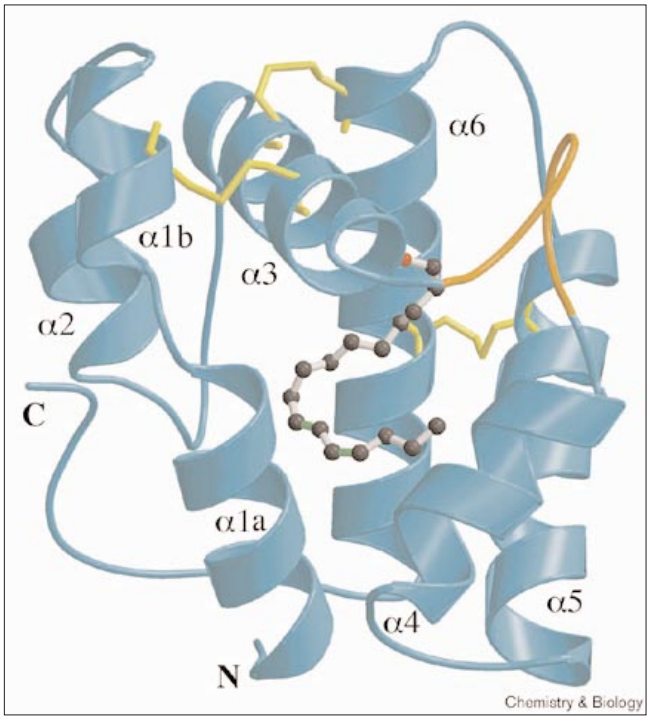

Overall structure of the *B. mori* PBP. Disulfide bridges are shown in yellow, and the loop covering the binding pocket (see text) is in orange. Bombykol is shown in a ball-and-stick representation with double bonds in green. The figure was prepared using BOBSCRIPT [36–38].

Figure 4

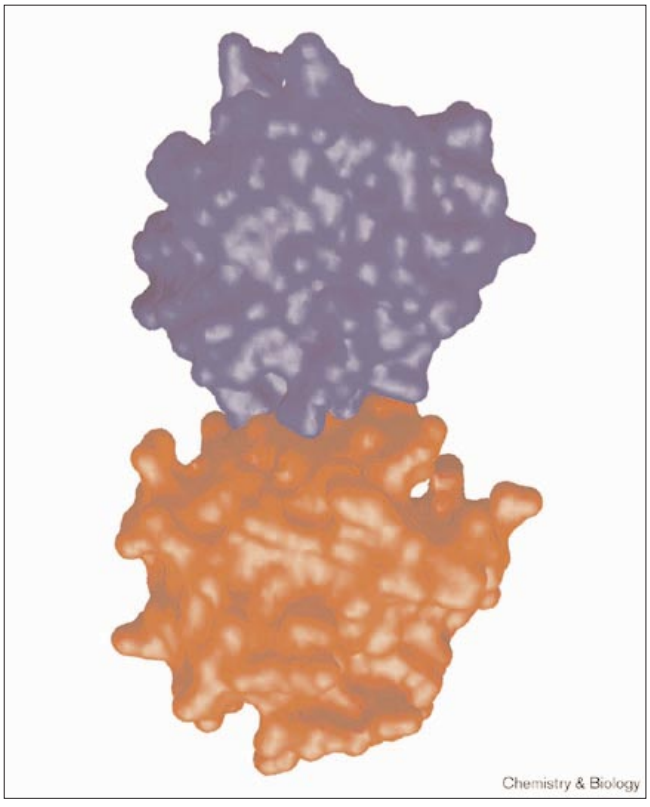

The dimer of *B. mori* PBP observed in the solid state. Monomers are in red and blue. The figure was prepared using GRASP [39].

dimerizing interactions. There were two PBP–PBP interactions that appeared relevant, and both involve roughly the same modest amount of surface area. The most extensive interaction was used to select the two monomers in the asymmetric unit, and this dimer interface involves 221 Å^2 of surface area (Figure 4) [18]. The dimeric interaction involves two different faces of the protein including a small hydrophobic patch around Pro64 from one monomer and Met131, Val133 and Lys38 of another, which are generally conserved residues. This dimer is not symmetric and would, in the limit, lead to aggregation, not dimerization. There is a symmetric PBP–PBP interaction at a crystallographic twofold axis with a contact area of 190 Å^2 [18]. The interacting surfaces do not involve hydrophobic contacts, however, and involve only two salt bridges (Lys38 and Asp132) and two hydrogen bonds (Ser130 and Lys6) of both monomers.

Bombykol-binding pocket

Bombykol is bound in a large flask-shaped cavity (Figure 5) with a tiny opening to the surface. Bound bombykol has a roughly planar hook-shaped conformation, and the outside (convex) part of bombykol interacts with numerous protein residues, whereas the inside (concave) part has few contacts (Figures 5,6). Residues from all parts of the protein contribute to the binding cavity (Figure 2).

The hydroxyl group of bombykol forms a hydrogen bond with the sidechain of Ser56 with an O–O distance of 2.8 Å (Figure 6). The conjugated double bonds of bombykol are sandwiched by Phe12 and Phe118 with the aromatic rings parallel to the molecular plane of bombykol and roughly 4.8 Å away (Figure 6). Both Phe12 and Phe118 are strongly conserved in the lepidopteran OBPs, and this conservation, along with their distance from bombykol, suggests that they form a general hydrophobic surface for binding and are not specificity determinants for bombykol's double bonds (Figures 2,6).

Of the residues involved in binding to bombykol, Met5, Phe12, Phe36, Trp37, Ile52, Ser56, Phe76, Val94, Glu98, Ala115 and Phe118 are highly conserved across lepidopteran OBPs (Figure 2), indicating that they are involved in the most general interactions with bound hydrophobic ligands. These residues are clustered above and below the approximate molecular plane of bombykol (Figure 6). Leu8, Ser9, Leu68, Leu90 and Thr111 are well conserved in the lepidopteran PBPs, but not in OBPs, and these residues are clustered in the plane of bombykol (Figure 6). The most variable residues, Met61, Leu62,

Figure 5

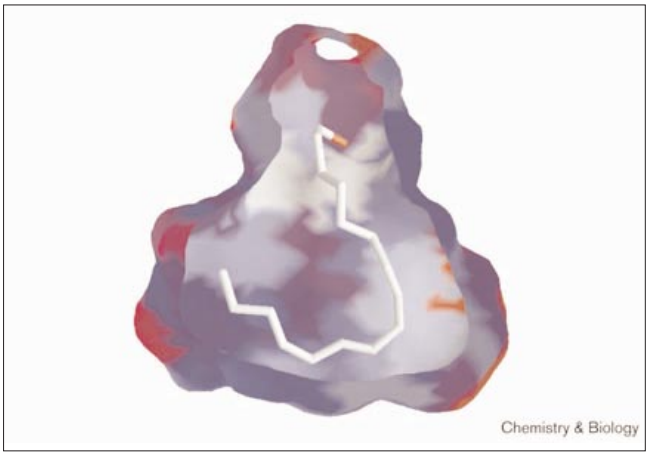

Cutaway view of bombykol in the binding pocket of *B. mori* PBP. Bombykol is shown as a stick figure with the hydroxyl oxygen in red. The pheromone-binding protein, part of which has been removed, is shown as a color-coded solid surface. White indicates a ligand–protein atomic distance of < 3 Å; blue, < 4.5 Å; and red, > 5.5 Å. The figure was prepared using GRASP [39] and modified in Adobe Photoshop.

Figure 6

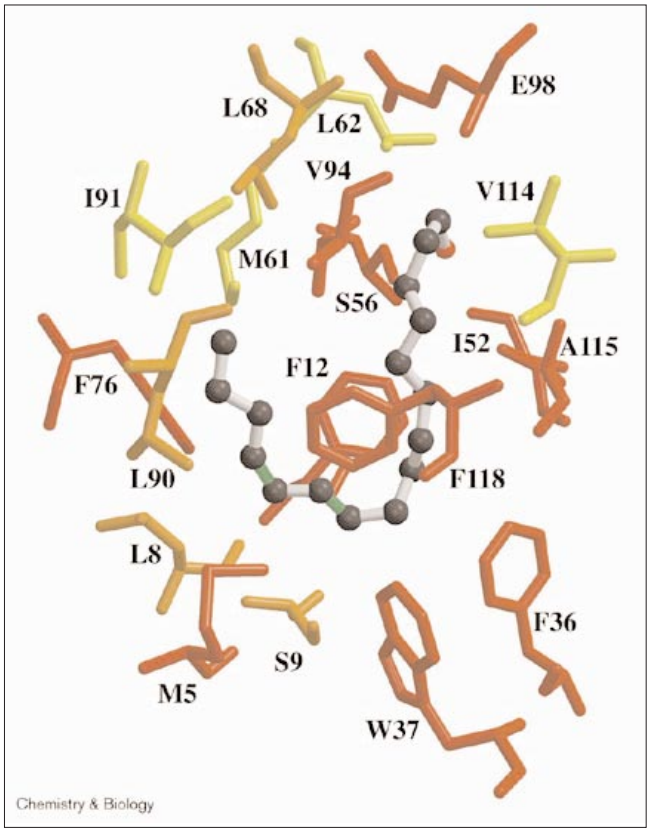

Another view of the bombykol binding pocket of *B. mori* PBP. Bombykol is at the center of the figure in ball-and-stick representation. The hydroxyl group is red, and the double bonds are green. Residues surrounding bombykol are shown in stick representation. Red denotes residues highly conserved across lepidopteran PBPs and GOBPs, residues in orange are conserved across PBPs but not GOBPs, and residues in yellow are the least conserved among lepidopteran PBPs. The figure was prepared using BOBSCRIPT [36–38].

Figure 7

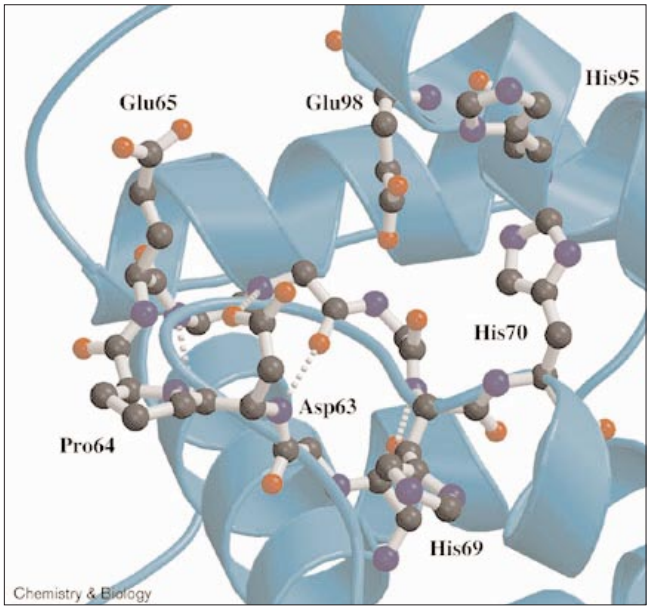

Close-up view of the loop covering the binding pocket. Sidechains are shown only for select residues (Asp63, Pro64, Glu65, His69, His70, His95 and Glu98). Hydrogen bonds are shown as dashed lines. The figure was prepared using BOBSCRIPT [36–38].

Ile91 and Val114, which are likely to be specificity binding determinants, are near the ends of the pheromone. In the OBPs, positions 62 and 114 are either valine, leucine, isoleucine or methionine, and this variability could be a way to alter the pocket at the oxidized end of the pheromone, and the same set of variations at positions 61 and 91 could serve the same purpose at the reduced end. The precise delineation of the roles of various residues in pheromone binding will require many additional studies, but the preliminary picture emerging from this structure has the most conserved/least discriminating residues forming the large hydrophobic surfaces above and below the molecular plane and the least conserved/most discriminating at either end of the bound ligand. The binding cavity appears to be most sensitive to the length of the pheromone as it circles the narrow wall of the binding pocket (Figure 5).

Bound bombykol is completely engulfed in PBP, and the structure doesn't clearly indicate how it enters or exits the binding pocket. The only part of bombykol that isn't surrounded by α helices is the hydroxyl end, which is covered by a loop running from residues 60–69 (Figures 2,7). This loop is held together in an approximate antiparallel β-strand conformation by three hydrogen bonds (Gly66N–Asp63O, Asp63N–Asn67O and His69N–Met61O; Figure 7). An additional interaction between the sidechain of Asp63 and the mainchain NH of Asn67 enforces this conformation. This relatively rigid lid is held in place by an interaction between the sidechain NH of Leu68 and the sidechain of Glu98. If this loop were not in place, the resulting opening would be adequate for bombykol's entrance and egress as discussed further below. This loop is also in a region of PBP, especially Pro64, involved in the dimeric interaction observed in the solid state (Figure 4).

pH-dependent conformational changes

A recent study on the PBP of *B. mori* indicates a reversible pH-dependent conformational change [14]. Both circular dichroism and fluorescence spectroscopy indicate a loss of rigid tertiary structure at low pH, and these observations suggest a rigid conformation at the neutral pH of the sensillary lymph and a partially unfolded conformation at the lower pH near a membrane surface [14]. The conformational transition takes place between pH 5 and 6 at ~pH 5.8. Additional experiments showed that *B. mori* PBP also undergoes a similar unfolding on interacting with model membranes [14]. A pH-dependent PBP conformation and the structural results described here suggest two possibilities for releasing bombykol.

Figure 8

Comparison of the NMR structure of the hydrophobic ligand-binding protein from *Tenebrio molitor* hemolymph, THP12 [19], and the PBP from *B. mori*. THP12 is on the left in yellow and PBP is on the right in cyan. The overall folds are similar but the α1 helix of PBP is mostly missing in THP12. The figure was prepared using BOBSCRIPT [36–38].

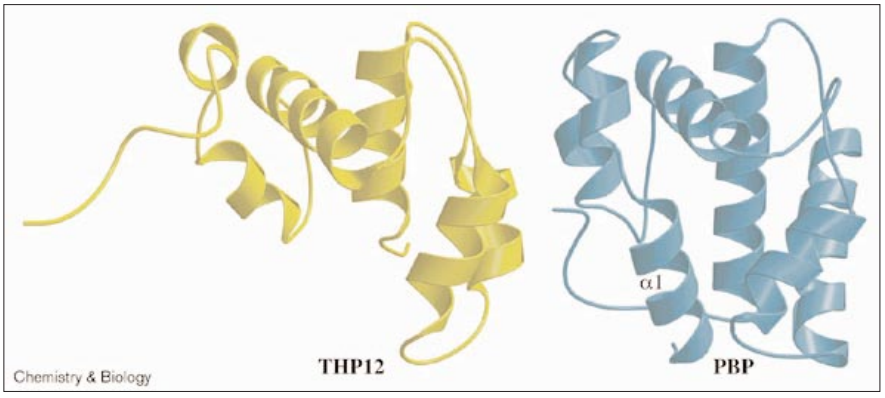

In the *B. mori* PBP structure, three histidine residues (His69, His70 and His95) that are strictly conserved across all known lepidopteran PBPs and GOBPs form a cluster at the base of the flexible loop near α4 (Figures 2,7). A pH drop from 6 to 5 would probably result in the protonation of one or more of these histidines, and the charge repulsion of the protonated histidines could destabilize the loop covering the binding pocket. In addition, protonated His69 and His70 could form salt bridges to Asp63 and Glu98, respectively, further destabilizing the closed conformation of the loop.

A more dramatic pH-induced conformational change is also possible, if less likely. As the pH is lowered, protonation of sidechains could result in destabilizing helices and a general unraveling of PBP's conformation. The resulting loss of secondary structure would open the binding pocket for release of pheromone.

The recently published structure of THP12 [19] suggests a specific way in which unraveling and release could be related. THP12 is a protein of unknown function from the mealworm *Tenebrio molitor* [19]. It has weak homology to the fruitfly (*Drosophila melanogaster*) PBP and no detectable homology to the *B. mori* PBP. However, the structure of THP12, which was determined by nuclear magnetic resonance (NMR) at pH 6.8, shows essentially the same fold as *B. mori* PBP (Figure 8). The most striking difference is that α1 in PBP is unwound in THP12, and the unraveling of α1 changes the hydrophobic pocket of PBP into the hydrophobic groove of THP12 (Figure 8) [19]. It is possible that the less rigid low-pH conformation of PBP resembles THP12. The α1 helix of *B. mori* PBP, especially its beginning, appears to have relatively few interactions with the rest of the protein, and its middle region is not perfectly helical (Figure 3).

A possible way to destabilize α1 involves protonation of His80, which is strictly conserved in all lepidopteran PBPs but is phenylalanine in lepidopteran OBPs (Figure 2). The sidechain of His80 is near Lys6 at the beginning of α1, and the charge repulsion might destabilize α1 enough to cause unraveling. Lys6 is strictly conserved in lepidopteran PBPs. The other histidine in PBP, His123, is also always histidine in lepidopteran PBPs and never histidine in lepidopteran GOBPs (Figure 2). Either model, opening a lid formed by the loop or unwinding of α1, would suffice to release bombykol from the protein.

A complete understanding of the significance of ligand release from PBP will require a fuller understanding of PBP's role in signal transduction. The specificity of pheromones for PBPs could mean that PBPs are not simply molecular ferries that discharge their cargo at the end of the journey but partners in a complex involving pheromone, pheromone receptor and pheromone-binding protein [1,13,9]. The solid-state structure of *B. mori* PBP illustrates how the loop covering the binding pocket can interact with another protein, and the residues of this loop are among the most variable in the PBPs.

Significance

The systematic study of chemical communications began in the 19th century with the observations of naturalists investigating the ability of female moths and butterflies to attract male mates [2]. These early experimenters demonstrated that communication took place over impressive distances — claims of several kilometers — and that males needed functional antennae to find females. Understanding the chemical basis of the communications took until the middle of the 20th century when the pioneering work of Butenandt's laboratory on the chemical structure and biological activity of bombykol firmly established the field of chemical communications [6]. Today we know a great deal about chemical communications, especially the sex pheromones of moths and butterflies. We know the structures of an almost bewildering number of pheromones, their biosynthesis, their biological activities, their laboratory synthesis and the biological activities of many analogs [3,4]. Our understanding of the small-molecule chemistry involved in chemical communications is extensive and thorough. Our understanding of how the information in a volatile organic molecule is transduced into an electrical signal from a nerve cell is neither extensive nor thorough and will require molecular and structural biology in addition to chemistry [1].

The current study reports the first structural characterization of a pheromone bound to its initial protein partner, a pheromone-binding protein. The pheromone, the silkworm moth pheromone bombykol in this case, is completely enclosed in a water-soluble protein. This encapsulation is needed both to transport the hydrophobic bombykol through the aqueous medium surrounding the nerve cell and to protect bombykol from destruction by the pheromone-degrading enzymes that assure that chemical signals don't linger. The specificity of the interaction between pheromone and pheromone-binding protein is just beginning to be understood, and the current study suggests that most of the specificity determinants are for the beginning and end of the linear pheromone chain and for its curvature in a bound conformation. The structure also suggests how pH-dependent conformational switches could function to release bound pheromone.

Materials and methods

Protein production and crystallization

B. mori PBP was overexpressed in *E. coli*, using the periplasmic expression system previously described [14]. The protein was released from the harvested cells by freeze and thaw cycles [20]. Selenomethionyl protein was expressed in a methionine auxotrophic strain of

Table 1

Data collection and refinement statistics.

Data collection				
	Native	MAD 1	MAD 2	MAD 3
Energy (keV)	13.574	12.675	12.679	14.000
Wavelength (Å)	0.9134	0.97818	0.97787	0.88560
Total observations	135,291	74,885	75,365	79,361
Unique reflections	26,466	7,378	7,370	7,744
Completeness	99.6%	95.1%	95.0%	100.0%
Anom. completeness		94.3%	94.2%	100.0%
Redundancy	5.1	10.1	10.2	10.2
R_{sym}	6.1%	8.9%	6.9%	7.3%
Resolution (Å)	1.8	2.8		
Selenium positions				
Expected	14			
Found	13			
Figure of merit				
Before density modification	0.621			
After density modification	0.926			
After phase extension	0.670			
Phasing power-isomorphous (anomalous)				
		MAD 1	MAD 2	MAD 3
Centric		2.228(0)	1.602(0)	0(0)
Acentric		4.065(3.795)	2.692(3.777)	0(3.594)
Space group	$P4_12_12$			
Cell constants	Native	$a = b = 53.18$ Å, $c = 191.54$ Å		
	SeMet	$a = b = 53.13$ Å, $c = 191.07$ Å		
Refinement				
$R_{working}$	21.8%			
R_{free}	27.5%			
Monomers per asymmetric unit	2			
Non-H protein atoms in asymmetric unit	2075			
Non-H ligand atoms in asymmetric unit	34			
Number of waters	210			
Ramachandran quality				
Core regions	94.7%			
Allowed regions	5.3%			
RMS deviations from ideality				
Bond lengths	0.012 Å			
Bond angles	2.4°			
Dihedral angles	22.1°			
Improper angles	1.9°			
Overall G-factor	–0.01			

E. coli [B834(DE3)] in M9 medium, containing 5 g/l glucose monohydrate, 2.5 mg/l of thiamin, 2 mg/l of biotin, 20 µM $ZnSO_4$, 10 µM $FeSO_4$, 50 mg/l of carbenicillin and 50 mg/l of seleno-L-methionine (Sigma). The cells were grown at 33°C to the mid-log phase (OD_{600} 0.6–0.7) and induced for 11–12 h with 1 mM isopropyl-β-D-trigalactopyranoside (IPTG). Purification steps were carried out as described previously, but the buffers contained 0.2 mM dithiothreitol and 1 mM EDTA to prevent oxidation of the protein [14]. Selenomethionine incorporation was determined by LC-ESI/MS. A stock solution of bombykol in ethanol (0.65 M) was mixed with 20 mg/ml protein in 10:1 molar ratio and incubated overnight at 4°C. Crystals of complex were obtained by the hanging drop method: drops of 2 µl protein complex and 2 µl reservoir solution were equilibrated at room temperature with a reservoir solution of 50% (w/v) PEG20,000 and 100mM Tris buffer, pH 8.2. Typical crystal dimensions were $0.06 \times 0.06 \times 0.5$ mm^3. Crystals of selenomethionyl protein were obtained in identical fashion.

Data collection

Crystals were protected for low temperature data collection in a mixture of 8% (v/v) 2*R*,3*R*-butanediol, 46% (w/v) PEG20,000 and 90 mM Tris, pH 8.2 and immediately flash frozen in liquid nitrogen. Native data were collected at MacCHESS station A-1 using an ADSC Quantum-4 detector [21]. MAD data were collected at the Argonne Advanced Photon Source beamline 14-BM-D, with an ADSC Quantum-4 detector [21]. All data were processed using the DPS/MOSFILM/CCP4 graphical interface [22–26]. Data collection statistics are given in Table 1. Heavy atom positions were determined using SHELXS [27], and heavy atom positions were refined and phases calculated using SHARP [28].

Model building and refinement

Model building was carried out in the program O [29]. Several rounds of simulated annealing and model rebuilding were performed in CNS

Figure 9

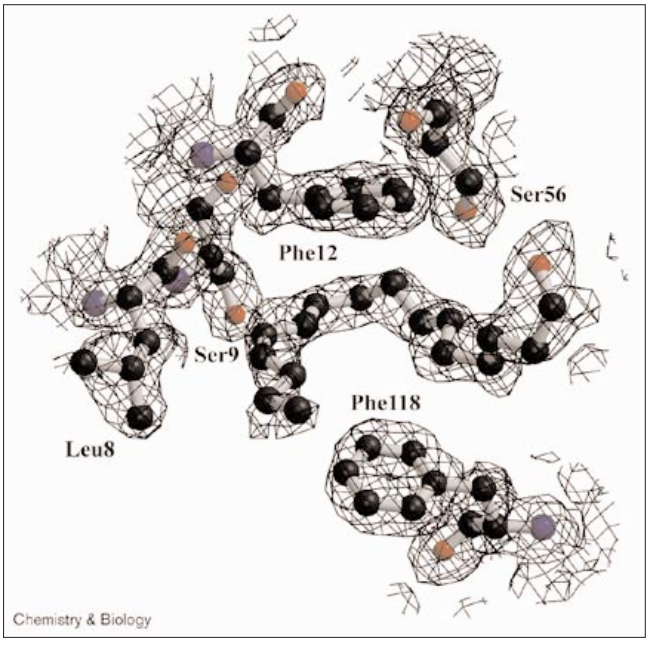

Electron density of bombykol and selected residues. The final atomic model is shown in ball-and-stick representation, and the $2F_o–F_c$ electron density is contoured at the 1.0 σ level. The figure was prepared using BOBSCRIPT [36–38].

[30] and O, followed by several rounds on maximum likelihood refinement using conjugate direction minimization in REFMAC [31] of the CCP4 suite [26.] Refinement was carried out using native data from a lowest resolution of 30 Å to a highest resolution of 1.8 Å with the native data set. Noncrystallographic symmetry (NCS) averaging was used in most stages of refinement and dropped when model building revealed substantial differences in the positions of the carboxy-terminal loops of the two monomers, at which point NCS averaging caused R_{free} to increase. Density modification was carried out in DM [32] of the CCP4 suite using NCS averaging, histogram matching and solvent flattening. Protein geometry was assessed using PROCHECK [33]. The electron density, especially in the hydrophobic core where bombykol is bound, was easily interpretable (Figure 9).

The final model contains residues 1–137 for both PBPs in the asymmetric unit. However, during refinement in REFMAC, occupancies were set to 0.01 for protein atoms for which no density was visible, thereby retaining geometric restraints on atom positions while effectively eliminating the contribution of those atoms to calculated structure factors. This procedure was imposed on some but not all of the sidechain atoms of Lys14, Lys38, Glu65, Glu75, Lys78, Glu84, Lys107, Lys124, Ser130, Asp132 and Val133 of monomer A, and Lys6, Leu10, Lys14, Asp17, Lys20, Lys21, Lys44, Asn45, Glu65, Lys107, Ile109 and Lys124 of monomer B.

Accession numbers

Coordinates have been deposited in the Protein Data Bank with accession code 1DQE.

Acknowledgements

This work was supported by the NIH (CA24487 to J.C. and a Molecular Biophysics Training Grant Award to B.H.S.) and the Japanese Program for Promotion of Basic Research Activities for Innovative Biosciences (W.S.L.). We thank Hubert Wojtasek for preliminary preparations of *B. mori* PBP, Habib Nasir for synthetic bombykol, Melanie Iwamoto for her assistance in growing crystals, Richard Gillilan of the Cornell Theory Center for help with graphics and molecular surface calculations, and the staff at the BioCARS beamline at the Advanced Photon Source (APS) for assistance in MAD data collection. The Cornell Theory Center is funded by the National Center for Research Resources (NIH). Use of the APS was supported by the U.S. Department of Energy, Basic Energy Sciences, Office of Science, under Contract No. W-31-109-Eng-38. Use of the BioCARS Sector 14 was supported by the National Institutes of Health, National Center for Research Resources, under grant number RR07707. This work is based upon research conducted at the Cornell High Energy Synchotron Source (CHESS), which is supported by the National Science Foundation under award DMR-9311772, using the Macromolecular Diffraction at CHESS (MacCHESS) facility, which is supported by award RR-01646 from the National Institutes of Health.

References

1. Krieger, J. & Breer, H. (1999). Olfactory reception in invertebrates. *Science* **286**, 720-723.
2. Agosta, W.C. (1992). *Chemical Communication: The Language of Pheromones*. Scientific American Library, New York.
3. Hansson, B.S. (1995). Olfaction in lepidoptera. *Experientia* **51**, 1003-1027.
4. Schneider, D. (1992). 100 years of pheromone research: an essay on lepidoptera. *Naturwissenschaften* **79**, 241-250
5. Butenandt, A, Beckmann, R., Stamm, D. & Hecker, E. (1959). Über den sexual-lockstoff des seidenspinners *Bombyx mori*. Reindarstellung and konstitution [On the sex attractant of the silkworm moth *Bombyx mori*. Isolation and structure]. *Z. Natuforsch. B* **14**, 283-284.
6. Hecker, E. & Butenandt, A. (1984). Bombykol revisited – reflections on a pioneering period and on some of its consequences. In *Techniques in Pheromone Research*. (Hummel, H.E. & Miller, T.A., eds), pp. 1-44, Springer Verlag, New York.
7. Kaissling, K.-E. & Priesner, E. (1970). Die riechschwelle des seidenspinners [The olfactory threshold of the silkworm moth]. *Naturwissenschaften* **57**, 23-28.
8. Vogt, R.G. & Riddiford, L.M. (1981). Pheromone binding and inactivation by moth antennae. *Nature* **293**, 161-163.
9. Pelosi, P. & Maida, R. (1995). Odorant-binding proteins in insects. *Comp. Biochem. Physiol. B Biochem. Mol. Biol.* **111**, 503-514.
10. Steinbrecht, R.A., Laue, M. & Ziegelberger, G. (1995). Immunolocalisation of pheromone-binding protein and general odorant-binding protein in olfactory sensilla of the silk moths *Antheraea* and *Bombyx*. *Cell Tissue Res.* **282**, 203-217.
11. Krieger, J., von Nickish-Rosenegk, E., Mameli, M., Pelosi, P. & Breer, H. (1996). Binding proteins from the antennae of *Bombyx mori*. *Insect Biochem. Mol. Biol.* **26**, 297-307.
12. Maida, R., Steinbrecht, A., Ziegelberger, G. Pelosi, P. (1993). The pheromone binding protein of *Bombyx mori*: purification, characterization, and immunocytochemical localization. *Insect Biochem. Mol. Biol.* **23**, 243-253.
13. Du, G. & Prestwich, G.D. (1995). Protein structure encodes the ligand binding specificity in pheromone binding proteins. *Biochemistry* **34**, 8726-8732.
14. Wojtasek, H. & Leal, W.S. (1999). Conformational change in the pheromone binding protein from *Bombyx mori* induced by pH and by interaction with membranes. *J. Biol. Chem.* **274,** 30950-30956.
15. Leal, W.S., Nikonova, L. & Peng, G. (1999). Disulfide structure of the pheromone binding protein from the silkworm moth, *Bombyx mori*. *FEBS Lett.* **464**, 85-90.
16. Spinelli, S., Ramoni, R., Grolli, S., Bonicel, J., Cambillau, C. & Tegoni, M. (1998). The structure of the monomeric porcine odorant binding protein sheds light on the domain swapping mechanism. *Biochemistry* **37**, 7913-7918.
17. Campanacci, V., Longhi, S., Nagnan-Le Meillour, P., Cambillau, C. & Tegoni, M. (1999). Recombinant pheromone binding protein 1 from *Mamestra brassicae* (MbraPBP1). *Eur. J. Biochem.* **264**, 707-716.
18. Vriend, G. (1990). WHAT IF: A molecular modeling and drug design program. *J. Mol. Graph.* **8**, 52-56.
19. Rothenmund, S., Liou, Y.-C., Davies, P.L., Krause, E. & Sönnichsen, F.D. (1999). A new class of hexahelical insect proteins revealed as putative carriers of small hydrophobic ligands. *Structure* **7**, 1325-1332.
20. Johnson, B.H. & Hecht, M.H. (1994). Recombinant proteins can be isolated from *E. coli* cells by repeated cycles of freezing and thawing. *Biotechnology* **12**, 1357-1360.
21. Szebenyi, D.M.E., Arvai, A., Ealick, S., Laluppa, J.M. & Nielsen, C. (1997). A system for integrated collection and analysis of crystallographic diffraction data. *J. Synchrotron Rad.* **4**, 128-135.

22. Nielsen, C., *et al.,* & Rossmann, M. (1998). DPS: A data processing system for oscillation method data from a 2X2 Mosaic CCD Detector. ACA Meeting July 18-23, Abstract 11.06.06.
23. Steller, I., Bolotovsky, R. & Rossmann, M.G. (1997). An algorithm for automatic indexing of oscillation images using Fourier analysis. *J. Appl. Crystallogr.* **30**, 1036-1040.
24. Bolotovsky, R., Steller, I. & Rossmann, M.G. (1998). The use of partial reflections for scaling and averaging x-ray area-detector data. *J. Appl. Crystallogr.* **31**, 708-717.
25. Leslie, A.G.W. (1990). Molecular data processing. In *Crystallographic Computing 5*. (Moras, D., Pojarny, A.D. & Thierry, J.C., eds), pp 50-61, Oxford University Press, Oxford.
26. Collaborative Computational Project, Number 4 (1994). The CCP4 suite: programs for protein crystallography. *Acta Crystallogr. D* **50,** 760-763.
27. Sheldrick, G.M. (1997). *SHELXL-97, a program for the refinement of crystal structures from diffraction data*. University of Göttingen, Göttingen, Germany.
28. De la Fortelle, E. & Bricogne, G. (1997). Maximum-likelihood heavy-atom parameter refinement for multiple isomorphous replacement and multiwavelength anomalous diffraction methods. *Methods Enzymol*. **276**, 472-494.
29. Jones, T.A., Zou, J.Y., Cowan, S.W. & Kjeldgaard, M. (1991). Improved methods for building protein models in electron density maps and the location of errors in these models. *Acta Crystallogr. A* **47,** 110-119.
30. Brünger, A.T., *et al.,* & Warren, G.L. (1998). Crystallography & NMR system: a new software suite for macromolecular structure determination. *Acta Crystallogr. D* **54**, 905-921.
31. Murshudov, G.N., Lebedev, A., Vagin, A.A., Wilson, K.S. & Dodson, E.J. (1999). Efficient anisotropic refinement of macromolecular structures using FFT. *Acta Crystallogr. D* **55**, 247-255.
32. Cowtan, K. (1994). *Joint CCP4 and ESF-EACBM Newsletter on Protein Crystallography* **31**, 34-38.
33. Laskowski, R.A., MacArthur, M.W., Moss D.S. & Thornton, J.M. (1993). PROCHECK: a program to check the stereochemical quality of protein structures. *J. Appl. Crystallogr.* **26**, 283-291.
34. Corpet, F. (1988). Multiple sequence alignment with hierarchical clustering. *Nucleic Acids Res.* **16**, 10881-10890.
35. Barton, G.J. (1993). Alscript: a tool to format multiple sequence alignments. *Protein Eng.* **6**, 37-40.
36. Kraulis, J.P. (1991). MolScript: A program to produce both detailed and schematic plots of protein structures. *J. Appl. Crystallogr.* **24**, 946-950.
37. Esnouf, R.M. (1997). An extensively modified version of MolScript that includes greatly enhanced coloring capabilities. *J. Mol. Graphics* **15**, 132-134.
38. Merritt, E.A. & Bacon, D.J. (1997). Raster3D: photorealistic molecular graphics. *Methods Enzymol*. **277**, 505-524.
39. Nicholls, A., Sharp, K. & Honig, B. (1991). Protein folding and association: insights from the interfacial and thermodynamic properties of hydrocarbons. *Proteins: Struct. Funct. Genet.* **11,** 281-296.

Because *Chemistry & Biology* operates a 'Continuous Publication System' for Research Papers, this paper has been published via the internet before being printed. The paper can be accessed from http://biomednet.com/cbiology/cmb – for further information, see the explanation on the contents pages.